Characterization of Sphingolipids from Mycopathogens: Factors Correlating with Expression of 2-Hydroxy Fatty Acyl (*E*)-Δ^3-Unsaturation in Cerebrosides of *Paracoccidioides brasiliensis* and *Aspergillus fumigatus*[†]

Marcos S. Toledo,[‡] Steven B. Levery,*[,§] Anita H. Straus,[‡] Erika Suzuki,[‡] Michelle Momany,[||] John Glushka,[§] J. Michael Moulton,[§] and Helio K. Takahashi*[,‡]

Department of Biochemistry, Universidade Federal de São Paulo/Escola Paulista de Medicina, Rua Botucatu 862, 04023-900, São Paulo, SP, Brasil, and Departments of Biochemistry and Molecular Biology and of Botany, and The Complex Carbohydrate Research Center, University of Georgia, 220 Riverbend Road, Athens, Georgia 30602

Received December 8, 1998; Revised Manuscript Received March 25, 1999

ABSTRACT: Significant differences exist between mammals and fungi with respect to glycosphingolipid (GSL) structure and biosynthesis. Thus, these compounds, as well as the cellular machinery regulating their expression, have considerable potential as targets for the diagnosis and treatment of fungal diseases. In this study, the major neutral GSL components extracted from both yeast and mycelium forms of the thermally dimorphic mycopathogen *Paracoccidioides brasiliensis* were purified and characterized by ^{1}H and ^{13}C NMR spectroscopy, ESI-MS and ESI-MS/CID-MS, and GC-MS. The major GSLs of both forms were identified as β-glucopyranosylceramides (GlcCer) having (4*E*,8*E*)-9-methyl-4,8-sphingadienine as long chain base in combination with either *N*-2′-hydroxyoctadecanoate or *N*-2′-hydroxy-(*E*)-3′-octadecenoate. The mycelium form GlcCer had both fatty acids in a ∼1:1 ratio, while that of the yeast form had on average only ∼15% of the (*E*)-Δ^3-unsaturated fatty acid. Cerebrosides from two strains of *Aspergillus fumigatus* (237 and ATCC 9197) expressing both GalCer and GlcCer were also purified and characterized by similar methods. The GalCer fractions were found to have ∼70% and ∼90% *N*-2′-hydroxy-(*E*)-3′-octadecenoate, respectively, in the two strains. In contrast, the GlcCer fractions had *N*-2′-hydroxy-(*E*)-3′-octadecenoate at only ∼20 and ∼50%, respectively. The remainder in all cases was the saturated 2-OH fatty acid, which has not been previously reported in cerebrosides from *A. fumigatus*. The availability of detailed structures of both glycosylinositol phosphorylceramides [Levery, S. B., Toledo, M. S., Straus, A. H., and Takahashi, H. K. (1998) *Biochemistry 37*, 8764−8775] and cerebrosides from *P. brasiliensis* revealed parallel quantitative differences in expression between yeast and mycelium forms, as well as a striking general partitioning of ceramide structure between the two classes of GSLs. These results are discussed with respect to possible functional roles for fungal sphingolipids, particularly as they relate to the morphological transitions exhibited by *P. brasiliensis*.

Occurrences of mycotic infections have increased dramatically during the last 2 decades, accompanied by a parallel increase in reports of resistance to available antifungal agents (*1*). In the process of developing models for fungal pathogenicity and establishing strategies for diagnosis and treatment, it is imperative to identify endogenous components which are not only critical to the fungal life cycle and infectivity, but which also contain structural elements distinct from those of the host (*1*, *2*). Any fungal components or metabolites which interact strongly with the host immune system are also of particular interest (*1*−*3*). Traditionally, a great many studies of immune response to antigens of pathogenic fungi, such as *Aspergillus fumigatus* and *Paracoccidioides brasiliensis*, have focused on protein, glycoprotein, and polysaccharide components of the cell wall, along with a variety of secreted fungal components (*4*−*6*). This is logical, since the cell wall is expected to be the primary locus for direct host−pathogen interactions. However, degradation of the fungal cell wall by host enzymes must necessarily lead to exposure of cell membrane antigens and, ultimately, the contents of the cytosol for processing, as evidenced by strong serological response to many of these components, including glycosphingolipids (*5*−*11*). Glycosphingolipids can be strongly immunogenic when associated with foreign proteins or with other cell membrane components (*12*); on the other hand, there is also evidence for significant immunosuppresive activity associated with certain glycosphingolipids (*13*). In addition to their potential as immunomodulatory agents, recent studies with *Saccha-*

[†] This work was supported by FAPESP, CNPq, and PRONEX (Brasil; M.S.T., E.S., A.H.S., and H.K.T.); a Burroughs Wellcome Fund New Investigator Award in Pathogenic Mycology (M.M.); a Glycoscience Research Award from Neose Technologies, Inc. (S.B.L.); and the National Institutes of Health Resource Center for Biomedical Complex Carbohydrates (NIH #5 P41 RR05351; S.B.L., J.G., and J.M.M.).

* Address correspondence to either S.B.L. or H.K.T. E-mail: leverysb@ccrc.uga.edu or takahashi.bioq@epm.br.

[‡] Department of Biochemistry, Universidade Federal de São Paulo/Escola Paulista de Medicina.

[§] Department of Biochemistry and Molecular Biology and The Complex Carbohydrate Research Center, University of Georgia.

[||] Department of Botany, University of Georgia.

10.1021/bi982898z CCC: $18.00
Published on Web 05/11/1999

romyces cerevisiae have pointed to key functional roles played by sphingolipids in the fungal life cycle, and deepened our understanding of the biosynthetic pathways and mechanisms for regulation of sphingolipid expression (*14*, *15*). However, the full extent to which these studies are applicable to various classes of mycopathogens remains to be determined.

As part of a program to elucidate possible functional roles of sphingolipids in the growth, life cycle, or infectivity of mycopathogens, as well as to understand their contribution to host immune response, we have undertaken systematic isolation and detailed characterization of both glycosylinositol phosphorylceramides (GIPCs)[1] and cerebrosides (monohexosylceramides) from a number of fungi, including pathogenic strains of *P. brasiliensis* and *A. fumigatus*. Cerebrosides containing (4*E*,8*E*)-*N*-2′-hydroxyalkanoyl- or (4*E*,8*E*)-*N*-2′-hydroxy-(*E*)-3′-alkenoyl-9-methyl-4,8-sphingadienine as the ceramide component have been identified in a variety of higher fungi (*16*−*26*). The majority of fungi synthesize only glucocerebrosides, but among *Aspergillus* species the expression of galactocerebroside (*A. niger*), glucocerebroside (*A. oryzae*; *A. versicolor*; *A. fumigatus* strain NCPF 2140), or a mixture of both (*A. fumigatus* strain NCPF 2109) has been observed (*22*, *27*−*29*). The precise function of these characteristic cerebrosides in vivo is unclear, but Kawai and Ikeda (*16*, *17*, *19*, *21*, *30*) have reported that fungal glucocerebrosides or structurally similar analogues exhibited fruiting-inducing activity in bioassays with *Schizophyllum commune*. The activity was observed with fungal glucocerebrosides having h16:0-h18:0, but not h24:0, fatty acids (*16*, *19*); the intact 9-methyl-4,8-sphingadienine, but not the β-glucopyranosyl residue, was essential for activity (*17*, *21*). In addition, Sitrin et al. (*31*) reported that *Pachybasium* cerebrosides potentiated the antifungal activity of aculeacin against *Candida albicans*, and, more recently, fruiting body-inducing cerebrosides of *Ganoderma lucidum* were found to inhibit the activity of α-type replicative DNA polymerases from calf thymus, cauliflower inflorescence, and a test strain of *Coprinus cinereus*, a mushroom used for bioassays of fruiting-body induction in the study (*26*).

Among fungi pathogenic to humans, detailed structural information on these compounds is still rather sparse. Cerebrosides of *A. fumigatus* (two strains) and *A. versicolor* (*22*), of *S. commune* (*16*, *17*, *30*), and of *Fusarium solani* (*25*) have been well characterized; among dimorphic mycopathogens, only *C. albicans* (*24*) has been subjected to a detailed examination with respect to both yeast and mycelial forms. Only the yeast form cerebroside of *Sporothrix schenckii* (*32*) has been described, and the sphingosine moiety was not well characterized.

Previously we reported the complete structure elucidation of GIPCs from the thermally dimorphic *P. brasiliensis*, including that of an antigenic compound having a novel glycan structure (*33*). In this paper, we report on the detailed characterization of *P. brasiliensis* cerebrosides by 1- and 2-D ^{1}H and ^{13}C NMR spectroscopy, electrospray ionization mass spectrometry (ESI-MS), and component analysis by GC-MS. In comparing cerebrosides obtained from both yeast and mycelial forms, we observed a structural dimorphism with respect to unsaturation of the fatty acyl moiety which appeared to correlate with the transition between the two growth phases. In addition, although structures for cerebrosides from two strains of *A. fumigatus* have been published (*22*), our investigation of two different strains producing both galacto- and glucocerebrosides led to an observation, not previously reported, of ceramide fatty acyl dimorphism dependent on hexose structure.

MATERIALS AND METHODS

Fungal Isolates and Growth Conditions. *Paracoccidioides brasiliensis* strain Pb18 was provided by Dr. C. Fava-Netto, Sao Paulo, SP, Brazil; strain B339 was provided by Dr. A. Restrepo-Moreno, Medellin, Columbia. Yeast and mycelial forms of the *P. brasiliensis* were grown at 37 and 23 °C, respectively, in YPD (peptone 5 g/L, glucose 15 g/L, yeast extract 5 g/L) using 2.5 L Fernbach flasks in a shaker at 100 rpm. After 1 week, both yeast and mycelium forms were inactivated with 0.1% of thimerosal, and after an additional 48 h, the fungi were collected by filtration on Whatman no. 1 filter paper. *Aspergillus fumigatus* (ATCC strain 9197) mycelia were grown in malt extract (20 g/L) at 25 °C using the same schedule and protocols for growth, inactivation, and collection as described. *A. fumigatus* strain 237, originally cultured from open lung biopsy from a patient with invasive pulmonary aspergillosis at Hope Hospital (Manchester, U.K.), was the gift of Dr. David W. Holden (Hammersmith Hospital, London, U.K.). Mycelia of strain 237 were grown from 1.25×10^9 spores at 37 °C on YPD medium in a shaker at 200 rpm over 24 h, filtered, and processed as described.

Extraction and Purification of Glycosphingolipids. Glycosphingolipids were extracted by homogenizing yeast or mycelium forms (25−35 g) in an Omni-mixer (Sorvall Inc., Wilmington, DE), 3 times with 200 mL of 2-propanol/hexane/water (IHW, 55:20:25, v/v/v, upper phase discarded), and twice with 200 mL of chloroform/methanol (CM, 2:1, v/v) as described (*34*, *35*). The five extracts were pooled, dried on a rotary evaporator, dialyzed against water, lyophilized, resuspended in chloroform/methanol/water (30:60:8, v/v/v; solvent A), and applied to a column of DEAE-Sephadex A-25 (Ac^- form). Neutral glycosphingolipids were eluted with 5 volumes of solvent A. Acidic glycosphingolipids were eluted with 200 mM sodium acetate in methanol. The neutral glycosphingolipid fraction was further purified from other contaminants by chromatography on silica gel 60 using a stepwise gradient of chloroform/methanol from 9:1 to 1:1 (v/v) (*36*). Fractions containing ceramide monohexosides (CMHs), as assessed by HPTLC analysis on silica gel 60 plates (E. Merck, Darmstadt, Germany) using solvent B (chloroform/methanol/water, 60:40:9 v/v/v, containing 0.002% w/v $CaCl_2$) as mobile phase and detection with Bial's orcinol reagent, were pooled, dried, and further purified by preparative-scale HPTLC using solvent B. Separated glycosphingolipid bands were visualized under UV light after

[1] Abbreviations: NMR, nuclear magnetic resonance spectroscopy; TOCSY, total correlation spectroscopy; HSQC, heteronuclear single quantum correlation; HMBC, heteronuclear multiple bond correlation; HPLC, high-performance liquid chromatography; HPTLC, high-performance thin-layer chromatography; GC, gas chromatography; ESI, electrospray ionization; EI, electron impact ionization; MS, mass spectrometry; CID, collision-induced decomposition; DMSO, dimethyl sulfoxide; TMS, trimethylsilyl; FAME, fatty acid methyl ester; CMH, ceramide monohexoside ≡ monohexosylceramide; GlcCer, β-glucosylceramide; GalCer, β-galactosylceramide; GIPC, glycosylinositol phosphorylceramide.

spraying with 0.01% primulin in 80% aqueous acetone. CMHs were isolated from silica gel scraped from the plates by repeated sonication in 2-propanol/hexane/water (55:20:25, v/v/v) followed by centrifugation. Following concentration of the extract, primulin was removed by passage through a short column of DEAE-Sephadex A-25 in solvent A. The purity of each fraction was assessed by HPTLC analysis as described above.

1- and 2-D Nuclear Magnetic Resonance Spectroscopy. Samples of underivatized CMH (~0.7−1.2 mg) were deuterium-exchanged by repeated evaporation from $CDCl_3$/CD_3OD (2:1 v/v) under a N_2 stream at 37 °C, and then dissolved in 0.5 mL of DMSO-d_6/2% D_2O (*37*−*39*) for NMR analysis.[2] 1-D ^1H NMR, 2-D $^1H-^1H$ TOCSY (*31*, *40*), and ^1H-detected, ^{13}C-decoupled, phase-sensitive, gradient (*41*) $^{13}C-^1H$ HSQC (*42*) and HMBC (*43*, *44*) experiments were performed at 35 °C on a Varian Unity Inova 600 MHz spectrometer using standard acquisition software available in the Varian VNMR software package. Proton-decoupled 1-D ^{13}C NMR spectra were acquired by direct detection on a Varian Unity Inova 500 MHz spectrometer under identical conditions.

Quantitation of (E)-Δ³-Unsaturated versus Saturated 2-Hydroxy-N-acylation. The percentage of (*E*)-Δ^3-unsaturation was calculated from the integrated ratios of the vinyl proton resonances corresponding to H-4″ of (*E*)-Δ^3-unsaturated fatty acid and H-5 of the sphingosine moiety. These resonances were chosen since they have similar splitting patterns and chemical shifts, but are completely resolved from each other in all spectra; although the chemical shift of H-5 is slightly affected by the presence or absence of (*E*)-Δ^3-unsaturation, the total integral for this resonance was assumed to represent 1.00 mol, regardless of fatty acyl distribution. In the case of the *A. fumigatus* low-Rf component, in which some residual high-R_f CMH was usually detected, a weighted component for this impurity was subtracted from the total (*E*)-Δ^3-unsaturation detected in the spectrum; this correction was taken as a simple function of the percentage of high-R_f CMH in the mixture, calculated from the relative integrals of the corresponding anomeric proton signals, and the percentage of (*E*)-Δ^3-unsaturation found in the pure high-R_f CMH from the same strain.

Electrospray Mass Spectrometry and Gas Chromatography−Mass Spectrometry. ESI-MS and tandem ESI-MS/CID-MS were performed in the positive ion mode on a PE-Sciex (Concord, Ontario, Canada) API-III spectrometer, using direct infusion of CMH samples dissolved in 100% MeOH containing 1 mM ammonium acetate, under conditions similar to those described previously (*33*). Generally, the mass range *m*/*z* 100−1000 was scanned in 0.1 u steps, with an orifice potential (OR) of 130 V (*m*/*z* 100−800, 0.25 u steps, OR = 200 V for MS-CID-MS experiments). Analysis of fatty acid components by GC-MS following acidic methanolysis, hexane extraction, and derivatization with Tri-Sil (Pierce, Rockford, IL) was carried out as described (*33*).

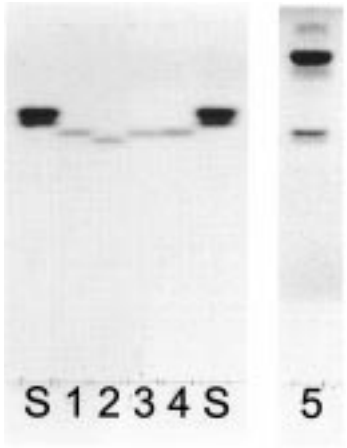

FIGURE 1: HPTLC analysis of CMH fractions from *A. fumigatus* strain 9197, upper and lower bands (lanes 1, 2), and from *P. brasiliensis* strain Pb18, yeast and mycelium forms (lanes 3, 4), compared with GlcCer from Gaucher's spleen (lanes S). A separate analysis of a crude neutral lipid fraction containing CMH from *A. fumigatus* strain 237 is presented for comparison in lane 5.

RESULTS

Isolation of Cerebroside Fractions from P. brasiliensis and A. fumigatus. HPTLC analysis of neutral (DEAE pass-through) lipids extracted from both yeast and mycelial forms of *P. brasiliensis* (strains Pb18 and B339) showed a single major orcinol positive band from each having an R_f value consistent with monohexosylceramide (CMH). Their R_f values (0.62) were identical to each other and slightly below that of GlcCer from Gaucher's spleen. On the other hand, similar preparations from hyphae of *A. fumigatus* (strains 237 and ATCC 9197) had two such bands, one with an R_f value identical to that of the *P. brasiliensis* CMH bands, and the other slightly below (R_f 0.60), consistent with the presence of both GlcCer and GalCer, as reported by Villas Boas et al. (*22*) for a different strain of *A. fumigatus* (NCPF 2109). Interestingly, while strain NCPF 2109 was reported to express GalCer and GlcCer in a ~1:1 ratio, in ATCC 9197 the amount of GalCer (lower band) appeared to be somewhat less (~40% of the total, by orcinol staining), and in 237 this band was present in much lower amounts (~20% of the total). These neutral glycosphingolipids were further purified by a methodology avoiding acetylation/Florisil chromatography/deacetylation (*45*) in order to maximize yield and allow for analysis of the fungal CMHs as close as possible to their native composition and state. As far as possible, bias was avoided in marking bands on preparative HPTLC plates so as not to exclude significantly material at the leading or trailing edges. HPTLC analysis of four purified fractions, as well as of the crude CMH-containing fraction from *A. fumigatus* strain 237, is illustrated in Figure 1.

NMR Spectroscopic Characterization of P. brasiliensis and A. fumigatus Cerebrosides. Native glycosphingolipid fractions dissolved in DMSO-d_6/2% D_2O were characterized by a series of 1- and 2-D homonuclear and heteronuclear NMR experiments ($^1H-^1H$ TOCSY, NOESY; $^1H-^{13}C$ HSQC, HMBC) to assign and correlate as many ^1H and ^{13}C resonances as possible. The downfield regions of 1-D ^1H

[2] Although fungal cerebrosides have previously been characterized by 1-D ^1H, 1-D ^{13}C, and 2-D $^1H-^1H$ COSY NMR as native compounds in $CDCl_3/CD_3OD$ mixtures (*16*, *17*, *22*−*24*), and by 2-D $^1H-^1H$ and 2-D $^1H-^{13}C$ COSY NMR as per-*O*-acetylated compounds in $CDCl_3$ (*18*, *22*, *25*, *27*), we prefer to employ DMSO-d_6/2% D_2O for NMR studies of native glycosphingolipids, since this solvent has long proven to present superior solubility characteristics, spectral dispersion, and chemical shift reproducibility for these compounds without the need for derivatization (*37*−*39*, *69*, *70*).

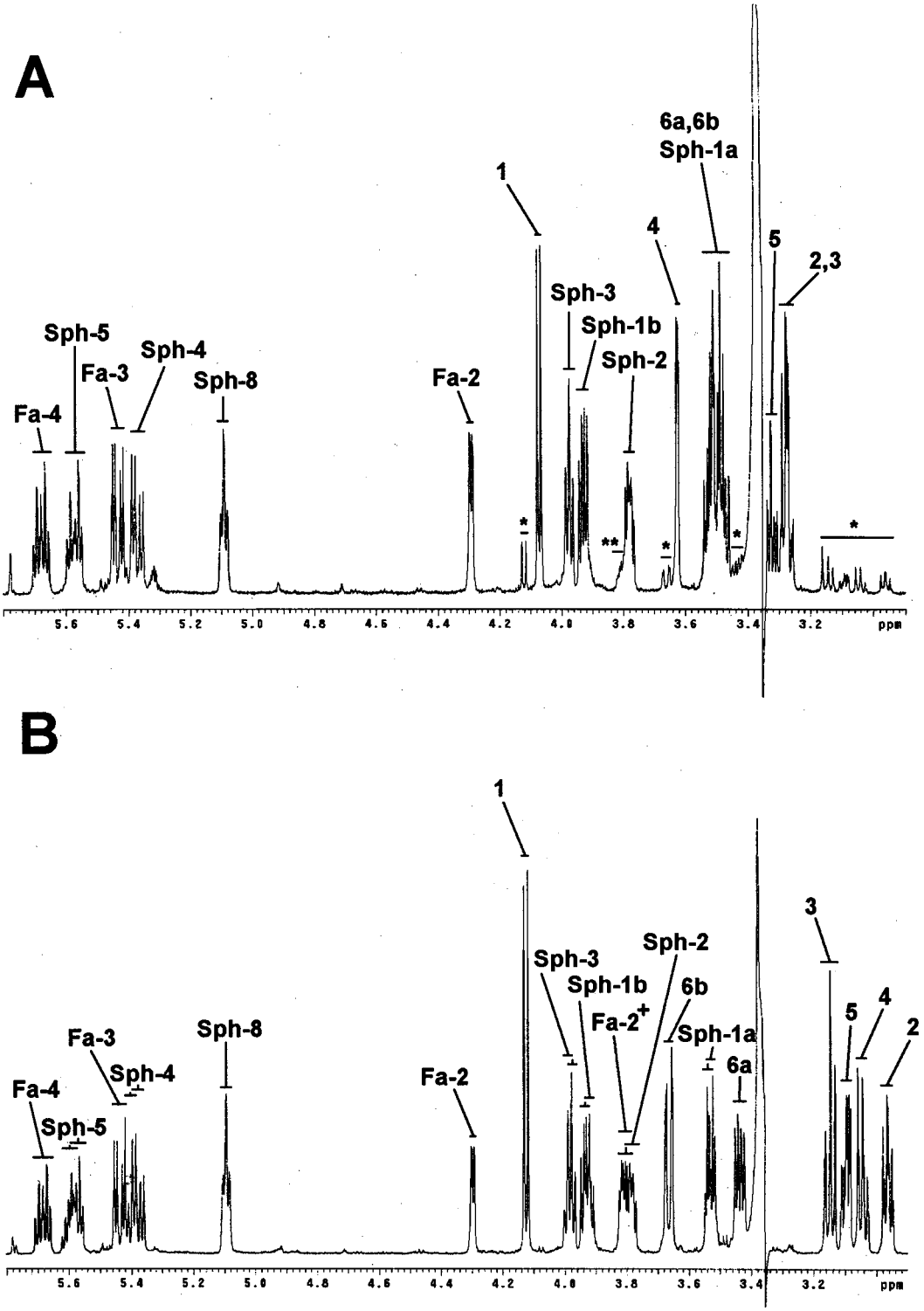

FIGURE 2: Downfield sections of 1-D ^{1}H NMR spectra of cerebroside (CMH) fractions from *A. fumigatus* strain 9197 (panel A, low-R_f CMH; panel B, high-R_f CMH). Resonances from nonexchangeable protons of sphingosine (Sph), fatty acyl (Fa), and hexose (prefix omitted) are designated by Arabic numerals. Resonances marked by one asterisk in panel A are from the hexose moiety high-R_f CMH component incompletely separated in preparative HPTLC (see panel B). The resonance marked by two asterisks is from Sph-2 of the minor CMH component having ceramide with saturated 2-hydroxy fatty acid. In panel B, two locations each are shown for Sph-1a,1b to Sph-5 corresponding to components having saturated and unsaturated 2-hydroxy fatty acid. Fa-2$^+$ is H-2 from saturated 2-hydroxy fatty acid, isochronous with the upfield Sph-2 resonance.

NMR spectra of *A. fumigatus* (strain 9197) and *P. brasiliensis* mycelium form (strain Pb18) and yeast form (strain B339) CMH fractions are reproduced in Figures 2 and 3. Preliminary analysis of these data led to the conclusion that both the *A. fumigatus* low-R_f CMH and the *P. brasiliensis* yeast form CMH are relatively homogeneous (~90% purity with respect to both glycosyl and ceramide moieties), while the *A. fumigatus* high-R_f CMH and the *P. brasiliensis* mycelium form CMH appeared to represent binary mixtures of similar composition, the two components of each differing solely with respect to structure of the ceramide moiety. Results of the 2-D ^{1}H−^{1}H and ^{1}H−^{13}C correlation NMR analysis,

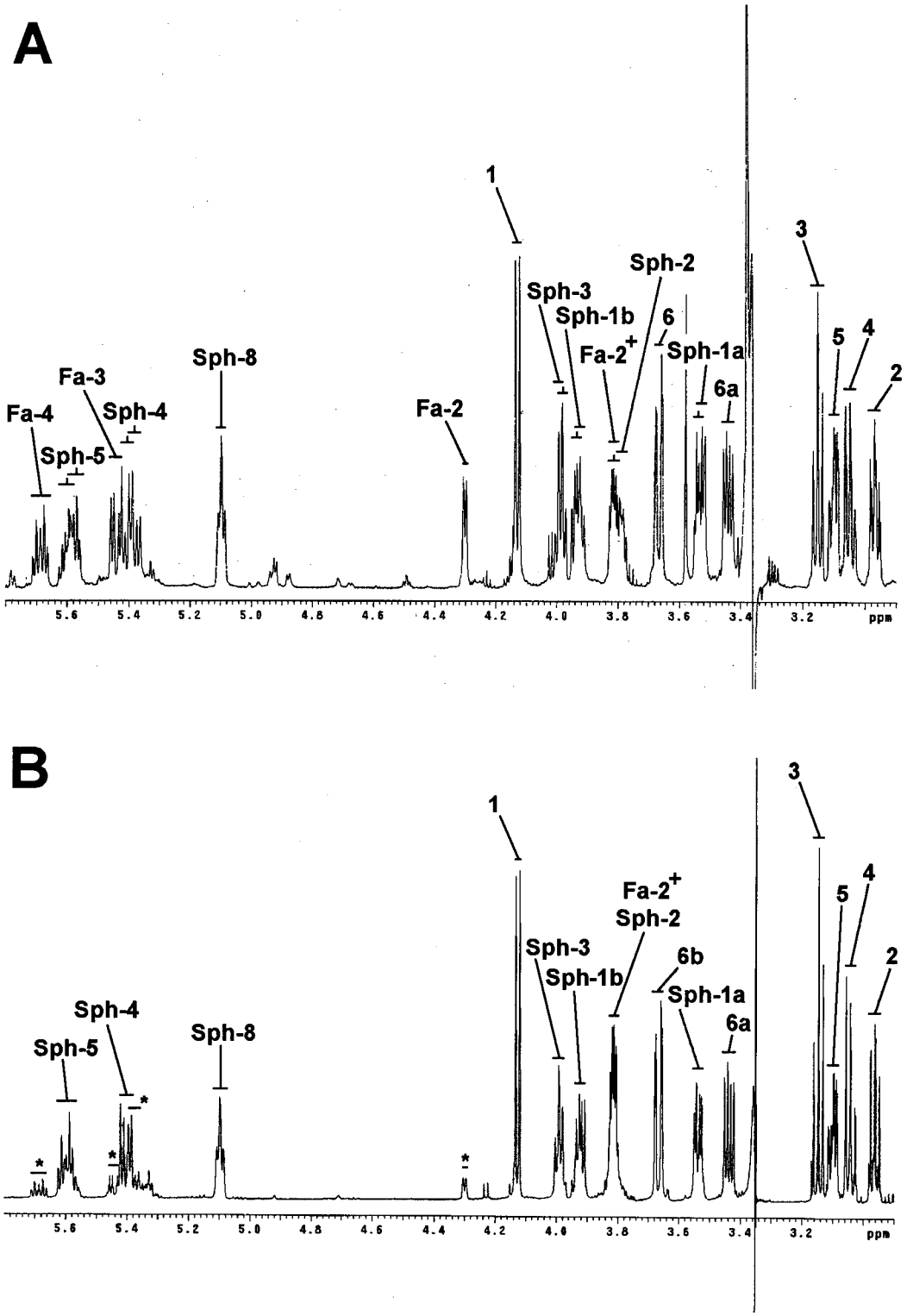

FIGURE 3: Downfield sections of 1-D ^{1}H NMR spectra of cerebroside fractions from *P. brasiliensis* (panel A, strain Pb18 mycelium form CMH; panel B, strain B339 yeast form CMH). All designations as in Figure 2, except resonances marked with an asterisk in panel B are from the component having ceramide with unsaturated 2-hydroxy fatty acid.

summarized in Tables 1 and 2, allowed for nearly complete characterization of all components involved, except for the precise chain lengths of the fatty acyl and sphingosine moieties. Key points of the analysis are as follows:

In the spectrum of the low-R_f *A. fumigatus* CMH (Figure 2A), the seven-proton spin system corresponding to a *β-galacto*pyranosyl residue was clearly recognized by its characteristic chemical shift and *J*-coupling patterns in both one and two dimensions in this medium (*39*). A key feature for recognition of a *β-galacto*pyranosyl spin system is the appearance of the H-4 signal, considerably narrowed as a result of its small *J*-couplings with both H-3 (∼2−3 Hz) and H-5 (<1.5 Hz). In the spectra of the other three fractions (Figures 2B and 3A,B), the seven-proton *β-gluco*pyranosyl spin system was similarly recognized (*38*) in both one and two dimensions (see TOCSY for the *P. brasiliensis* yeast

Table 1: ^{1}H Chemical Shifts (ppm) of Hexose (Hex), Sphingosine (Sph), and Fatty Acyl (Fa) Carbons of GalCer from Mycelia of *A. fumigatus* (A); of GlcCer from Mycelia of *P. brasiliensis* and *A. fumigatus* (both B + C); and of GlcCer from the Yeast Form of *P. brasiliensis* (C), in DMSO-d_6/2% D_2O at 35 °C[a]

		GalCer (A)	GlcCer (B)	GlcCer (C)
Hex-	1	4.079	4.128	4.127
	2	3.296	2.967	2.963
	3	3.288	3.150	3.147
	4	3.631	3.047	3.042
	5	3.332	3.101	3.099
	6a	3.480	3.441	3.436
	6b	3.531	3.667	3.667
Sph-	1a	3.507	3.533	3.537
	1b	3.936	3.931	3.922
	2	3.785	3.799	3.813
	3	3.981	3.988	3.987
	4	**5.377**	**5.381**	**5.404**
	5	**5.580**	**5.592**	**5.601**
	6	1.950	1.950	1.960
	7	1.978	1.978	1.985
	8	**5.098**	**5.098**	**5.098**
	10	1.922	1.921	1.920
	11	1.338	1.341	1.335
	12−16	1.234	1.234	1.234
	17	1.271	1.271	1.271
	18	0.853	0.853	0.853
	19	1.546	1.545	1.543
Fa-	2	4.300	4.301	3.813
	3a	**5.441**	**5.440**	1.437
	3b			1.570
	4	**5.686**	**5.687**	1.293
	5	1.961	1.961	1.234
	6	1.296	1.296	1.234
	7−16	1.234	1.234	1.234
	17	1.271	1.271	1.271
	18	0.853	0.853	0.853

[a] A, B, and C refer to structures drawn in Scheme 1. Vinylic carbons are in boldface for emphasis.

Table 2: ^{13}C Chemical Shifts (ppm) of Hexose (Hex), Sphingosine (Sph), and Fatty Acyl (Fa) Carbons of GalCer from Mycelia of *A. fumigatus* (A); GlcCer from Mycelia of *P. brasiliensis* and *A. fumigatus* (both B + C); and of GlcCer from the Yeast form of *P. brasiliensis* (C), in DMSO-d_6/2% D_2O at 35 °C[a]

		GalCer (A)	GlcCer (B)	GlcCer (C)
Hex-	1	104.43	103.78	103.78
	2	70.80	73.62	73.62
	3	73.54	76.71	76.71
	4	68.35	70.29	70.29
	5	75.58	77.15	77.15
	6	60.65	61.34	61.34
Sph-	1	68.76	68.82	68.98
	2	53.16	53.20	53.09
	3	70.80	70.79	70.82
	4	**131.19**	**131.16**	**131.28**
	5	**131.36**	**131.40**	**131.45**
	6	32.44	32.47	32.44
	7	27.60	27.57	27.57
	8	**123.84**	**123.83**	**123.81**
	9	**135.27**	**135.27**	**135.28**
	10	39.13	39.09	39.21
	11	27.60	27.63	27.68
	12−16	29.35	29.35	29.32
	17	22.36	22.44	22.38
	18	14.19	14.24	14.21
	19	16.06	16.00	16.05
Fa-	1	172.35	172.39	174.09
	2	72.20	72.22	71.30
	3	**129.32**	**129.29**	34.71
	4	**131.36**	**131.40**	24.80
	5	31.92	31.92	29.32
	6−16	29.35	29.35	29.32
	17	22.36	22.44	22.38
	18	14.19	14.24	14.21

[a] A, B, and C refer to structures drawn in Scheme 1. Vinylic carbons are in boldface for emphasis. All assignments were made from correlations in ^{1}H-detected ^{1}H−^{13}C gHSQC Spectra, but chemical shift values are those obtained from 1-D ^{13}C spectra, except for that of Sph-10, which overlapped the strong DMSO ^{13}C resonance in the 1-D spectra.

form CMH, Figure 4A). Resonances from a small amount of the residual GlcCer component are also visible in the 1-D spectrum of the *A. fumigatus* GalCer (Figure 2A). ^{1}H-detected ^{1}H−^{13}C HSQC spectra allowed assignment of all corresponding ^{13}C resonances (Table 2). In ^{1}H-detected ^{1}H−^{13}C HMBC spectra (illustrated for the *A. fumigatus* 9197 GalCer, Figure 5), the β-Hex H-1/Cer C-1 and β-Hex C-1/Cer H-1a,b correlations defined the glycosidic linkage without resorting to chemical shift/structure reporter group arguments. These results confirm the expression of both GalCer and GlcCer in this strain of *A. fumigatus*, and similar spectra were obtained for CMH fractions from strain 237. On the other hand, both yeast and mycelial forms of *P. brasiliensis* appear to express GlcCer exclusively.

Starting from C-1/H-1a/H-1b of the aglycon, analysis of 2-D ^{1}H−^{1}H and ^{1}H−^{13}C correlation NMR data next allowed sequential assignment of both ^{1}H and ^{13}C resonances in each spectrum with respect to the sphingosine moiety. The pattern in all fractions was consistent with a (4*E*,8*E*)-9-methyl-4,8-sphingadienine structure; characteristic features are the pair of vinyl resonances for the (*E*)-Δ^4-unsaturation, which is found in glycosphingolipids from many species including mammals, and the single vinyl resonance (5.098 ppm) for the (*E*)-Δ^8-unsaturation where C-9 is substituted with a methyl group (1.545 ppm), features which are not found in mammalian sphingosines, but are characteristic of cerebrosides from fungi and some marine invertebrates. The connectivity between these two unsaturations is easily found via the allyl CH_2 resonances for C-6 and C-7 in homonuclear *J*-correlated experiments on *P. brasiliensis* yeast form GlcCer (TOCSY, Figure 4A), but the continuation to C-10 from C-8 cannot be reliably established without the use of heteronuclear correlation experiments, since C-9 has no proton attached, and there is no apparent H-8/H-10 *J*-coupling, even at long mixing times. The HMBC experiment (Figure 5) clearly demonstrated the necessary connectivities between C-8/H-8, C-9, C-19/H-19, and C-10/H-10; and from there to the bulk CH_2 resonance via C-11/H-11. Our assignments for C-18 (14.21 ppm) and C-19 (16.05 ppm) are consistent with those previously made on both peracetylated (*22*) and native (*23*) samples; the *E* configuration for Δ^8-unsaturation has been previously assigned based on the chemical shift of C-19 (*23*), as well as by observation of nuclear Overhauser enhancement of H-8 upon irradiation of H-10 (*22*).

Analysis of the fatty acyl spin systems begins conveniently with H-2″/C-2″, observed at 3.813/71.30 ppm for the yeast form *P. brasiliensis* GlcCer and at 4.301/72.22 ppm for GalCer of *A. fumigatus*. In the latter case, proton connectivities could be followed directly (see TOCSY, Figure 4B) through a pair of vinyl resonances (5.441 and 5.686 ppm), again with coupling patterns characteristic of the *E* configuration, to the bulk CH_2 resonance via H-5″ and H-6″ (1.961

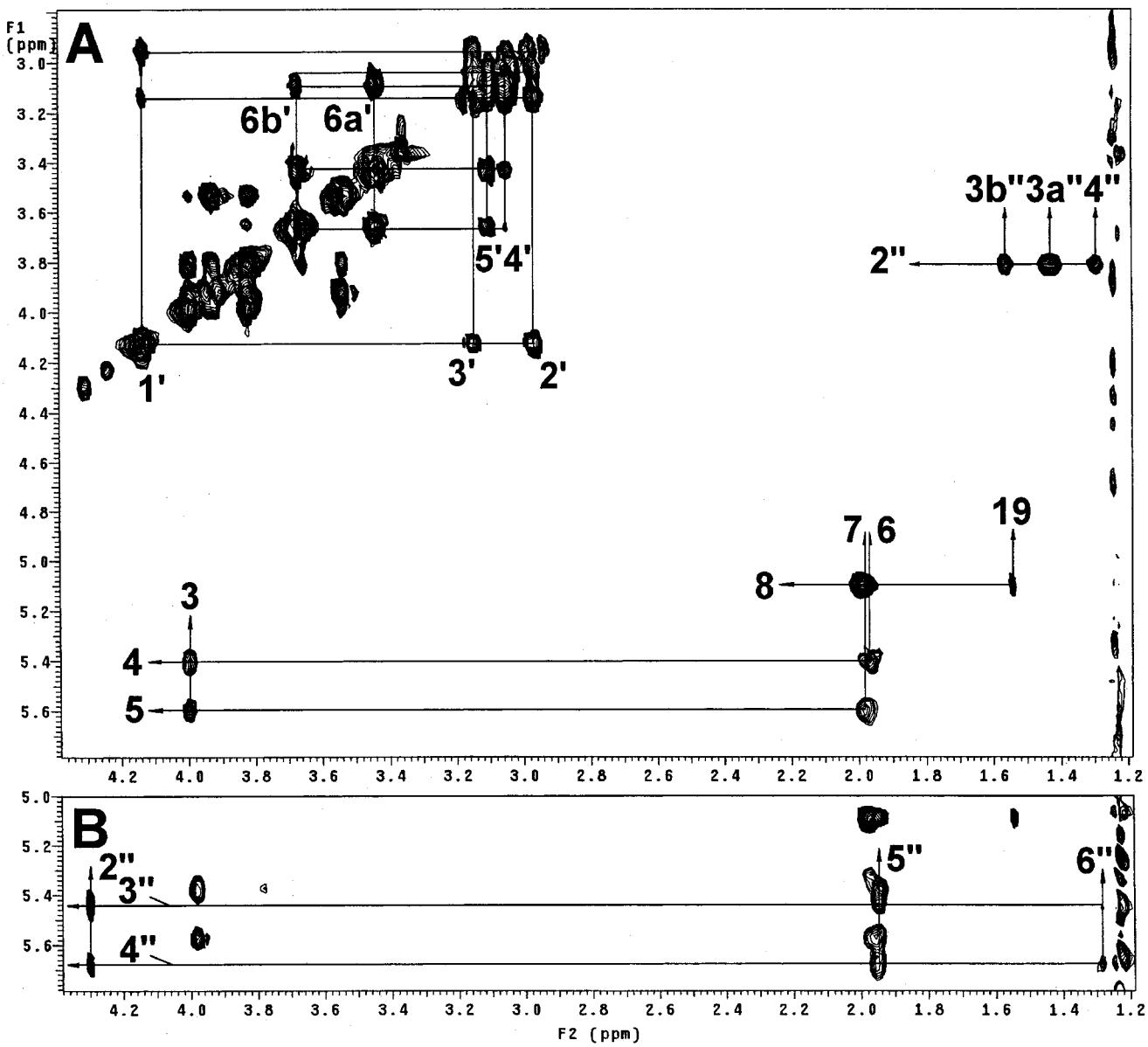

FIGURE 4: Sections of TOCSY spectra of yeast form cerebroside from *P. brasiliensis* strain B339, showing correlations for β-*gluco*pyranosyl (1′−6b′), sphingosine (3−8, 19), and saturated 2-hydroxy fatty acid (2″−4″) spin systems (panel A); and of low-R_f cerebroside from *A. fumigatus* strain 9197, showing alternate set of correlations for the unsaturated 2-hydroxy fatty acid (2″−6″) spin system (panel B).

and 1.316 ppm, respectively). These connectivities could also be confirmed by long-range proton/carbon correlations in the HMBC spectrum (Figure 5). Long-range proton/carbon correlations could also be followed in the other direction, via the H-3″/C-1″ correlation (5.441/172.35 ppm), and from there across the amide linkage to the sphingosine moiety via Fa-C1/Sph-H2 (see Figure 5). An interesting (and useful) interchain shielding effect of *N*-acyl Δ^3-unsaturation on H-4 and H-5 of the sphingosine moiety was clearly observed ($\Delta\delta \cong -0.03$ and -0.02 ppm, respectively).

Since the bulk CH_2 resonance (1.234 ppm), representing the carbons between the terminal methyls (0.853 ppm) and the functionalized groups, is difficult to integrate precisely, and in any case represents a composite total for which there is no basis for assigning a specific distribution between the acyl and sphingosine alkyl chains, these features were defined by ESI-MS and fatty acid component analysis via degradation, derivatization, and GC/MS, as described in later sections.

Quantitation of (E)-Δ^3-Unsaturated versus Saturated 2-Hydroxy-N-acylation. With assignments in hand for the ^{13}C and ^1H resonances characteristic for both the saturated and the (*E*)-Δ^3-unsaturated 2-hydroxy-*N*-acyl groups, it was clear that the *A. fumigatus* strain 9197 GlcCer and the *P. brasiliensis* strain Pb18 mycelium form GlcCer were mixtures containing approximately 40−60% each of the saturated *N*-acyl form and the (*E*)-Δ^3 *N*-acyl form. On the other hand, the *P. brasiliensis* yeast form GlcCer from both strains appeared to contain significantly smaller amounts of the (*E*)-Δ^3 form, based on the amplitude of resonances for H-2″ at 4.301 ppm and H-4″ at 5.686 ppm in the spectra. By the same criteria, the *A. fumigatus* strain 9197 GalCer fraction contained only small amounts of the saturated *N*-acyl form. Quantitation of the relative amounts of (*E*)-Δ^3 form in each fraction (Table 3), based on integration of the H-4″ resonance relative to that for H-5 at 5.580 ppm, gave the following approximate average percentages: *A. fumigatus* strain 9197 GlcCer, 51%; GalCer, 92%; *P. brasiliensis* strain Pb18

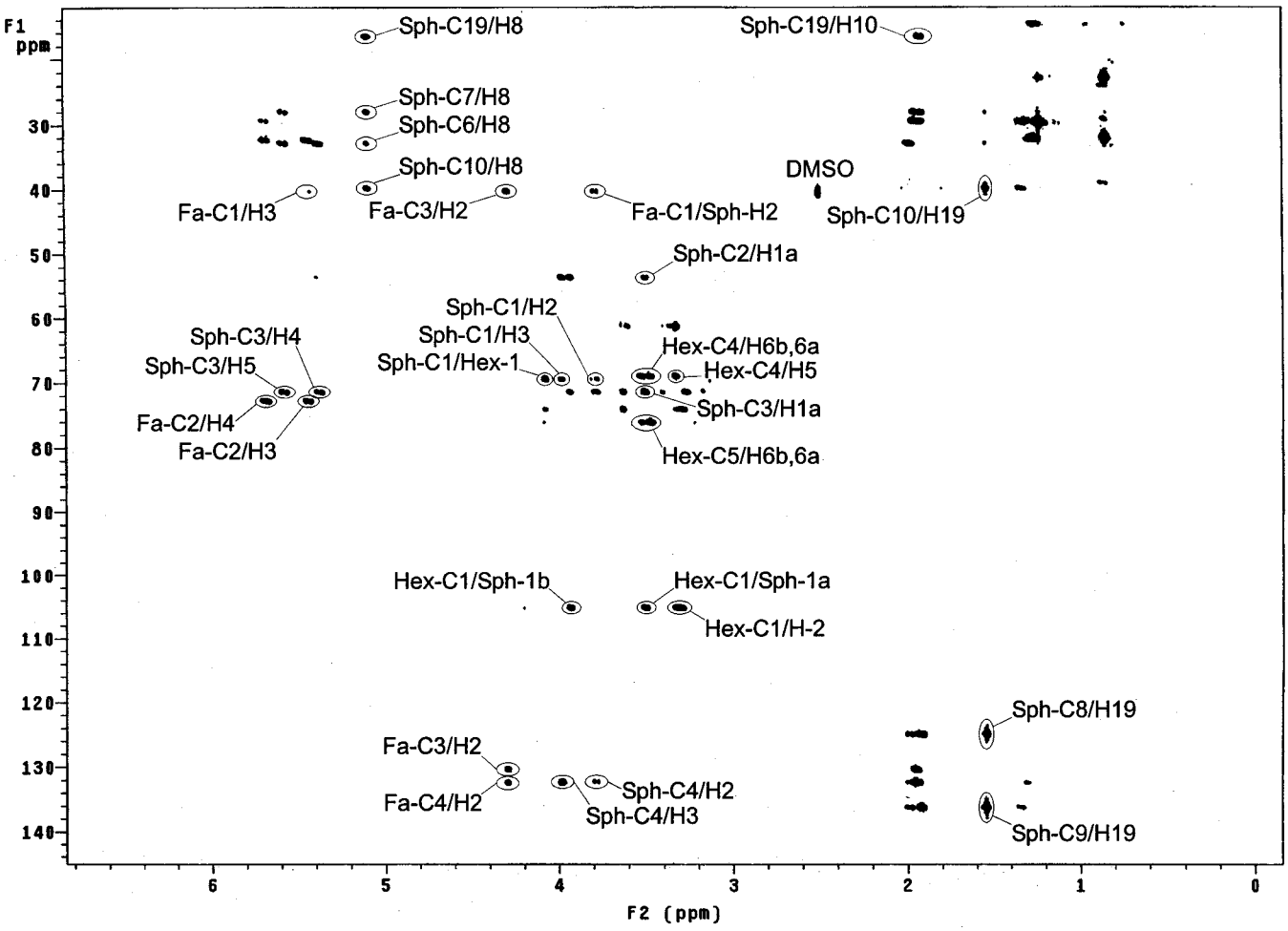

FIGURE 5: ^{1}H-detected $^{1}H-^{13}C$ heteronuclear multiple bond correlation (HMBC) spectrum of GalCer from *A. fumigatus* strain 9197, showing key long-range correlations (cross-peaks marked by ovals), including glycosidic H1′−C1′−O1′−C1 and C1′−O1′−C1−H1a,H1b correlations with the sphingosine moiety, and the amide H2−C2−N2−C1″ correlation between sphingosine and the fatty acyl moiety (the C1″ [Fa-C1] correlations are folded with respect to F1 due to limitation of the ^{13}C sweep width). Unmarked cross-peaks are all intraresidue or intrachain correlations.

Table 3: Mole Percent of Δ^3-Unsaturation of C18 2-Hydroxy Fatty Acid in Different Preparations of Cerebrosides from *P. brasiliensis* (*P.b.*) and *A. fumigatus* (*A.f.*) with Respect to Strain, Growth Phase, Hexose Moiety, and Medium, Based on Relative Integration of Resonances for Fa-H4 (5.686 ppm) and Sph-H5 (5.580 ppm) in 1-D NMR Spectra

species	strain	phase	medium	hexose	% Δ^3	av (no.)
P.b.	B339	Y[a]	SS[b]	Glc	2, 22, 14	13 (3)
P.b.	Pb18	Y	YPD	Glc	2, 30	16 (2)
P.b.	Pb18	M	YPD	Glc	53, 55	54 (2)
A.f.[c]	9197	M	ME	Glc	61, 40	51 (2)
A.f.	9197	M	ME	Gal	92, 92	92 (2)
A.f.	237	M	YPD	Glc	23, 14	19 (2)
A.f.	237	M	YPD	Gal	72, 73	73 (2)

[a] M = mycelial; Y = yeast. [b] SS = Sabouraud solid medium; ME = malt extract; YPD = yeast, peptone, glucose. [c] Monomorphic (mycelial only).

mycelium form GlcCer, 54%; strains B339 and Pb18 yeast form GlcCer, 13−16%. While the composition of *P. brasiliensis* yeast form GlcCer varied significantly from batch to batch, the amount of the (*E*)-Δ^3 form was not observed at a level higher than ∼30%, and in some batches this unsaturation was hardly detectable (≤2%). The most dramatic difference in composition was found in the *A. fumigatus* 237 CMH fractions, with the GlcCer fraction having >50% less (*E*)-Δ^3-unsaturation than the GalCer fraction.

Mass Spectrometric Characterization of P. brasiliensis and A. fumigatus Cerebrosides. In Figure 6A are reproduced comparable segments of $^{+}$ESI mass spectra of underivatized cerebroside fractions from *A. fumigatus* strain 9197 and *P. brasiliensis* strain Pb18, showing pseudomolecular ion profiles from which ceramide type, size, and relative homogeneity can be inferred. In the spectrum of the GalCer fraction from *A. fumigatus*, for example, the predominant sodiated pseudomolecular ion at *m*/*z* 776 (Figure 6A, far left) corresponds to a nominal molecular mass of 753 Da, consistent with the published structure having (4*E*,8*E*)-*N*-2′-hydroxy-(*E*)-3′-alkenoyl-9-methyl-4,8-sphingadienine as the ceramide moiety (*22*). Although a number of fragments were observed in the spectral region below *m*/*z* 700 under these conditions (not shown), the presence of considerable noise and possible impurity peaks in the spectrum made interpretation somewhat ambiguous. However, acquisition of a $^{+}$ESI-MS/CID-MS experiment with selection of the pseudomolecular ion in Q1 (Figure 6B) furnished a product ion spectrum free of interferences, which confirmed that the fatty acyl group is 2-OH-octadec*en*oate (h18:1) and that (d19:2) 9-methylsphinga-4,8-dienine is the long-chain base, by

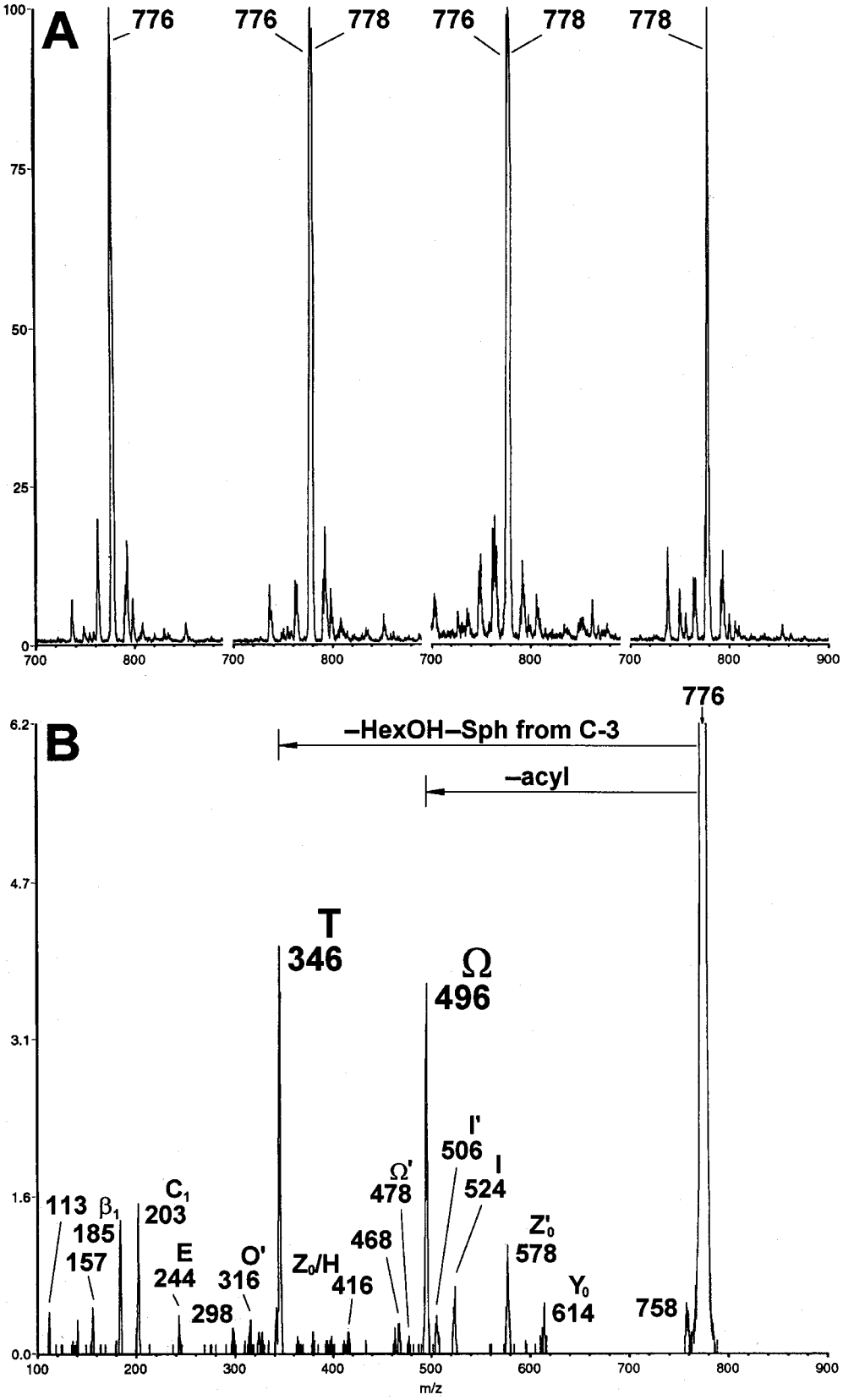

FIGURE 6: $^{+}$ESI mass spectrometry of cerebrosides from *A. fumigatus* and *P. brasiliensis*. Panel A, left to right: pseudomolecular ion regions of $^{+}$ESI-MS spectra for *A. fumigatus* strain 9197 low-R_f (GalCer) and high-R_f (GlcCer) cerebrosides, *P. brasiliensis* strain Pb18 mycelium form (GlcCer), and yeast form (GlcCer) cerebrosides, respectively. Panel B: $^{+}$ESI-MS/CID-MS product ion spectrum from $[M+Na]^{+}$ (*m*/*z* 776) of *A. fumigatus* low-R_f cerebroside.

virtue of the abundant $[M+Na - acyl]^{+}$ (Ω) and $[M+Na - HexOH - Sph\text{-}C_3{-}C_{19}]^{+}$ (T) fragments (*46*) at *m*/*z* 496 and 346, respectively.[3] Unlike the case with high-energy CID spectra, the triple quadrupole MS/MS spectra did not reliably furnish fragments showing the location of double bonds and other functionalities. However, these features, along with the

Scheme 1: Structures of *N*-2′-Hydroxyoctadec-3-enoyl-1-*β*-D-galactopyranosyl- (A), *N*-2′-Hydroxyoctadec-3-enoyl-1-*β*-D-glucopyranosyl- (B), and *N*-2′-Hydroxyoctadecanoyl-1-*β*-D-glucopyranosyl- (C) -9-Methyl-*trans*-4,*trans*-8-sphingadienines, with Numbering of Sphingosine Moiety[a]

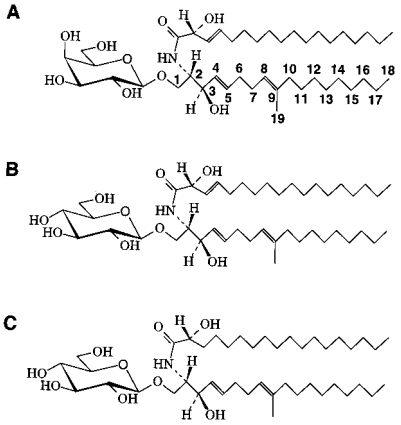

[a] Strains of *A. fumigatus* have been reported to express either a mixture of compounds A and B or compound B only (*22*), but compound C may also be synthesized in some strains (this work). Compounds B and C are the predominant monohexosylceramides extracted from the mycelium form of *P. brasiliensis*, while compound B was found in significantly higher proportions in the yeast form.

identities of the hexose residues, were deducible from the NMR data alone; owing to the complementary nature of the two analytical techniques, complete structures of all three major cerebroside molecular species (Scheme 1) present in the four fractions could be readily elucidated with a minimum expenditure of material.

Thus, in the spectrum of the GlcCer fraction from the yeast form of *P. brasiliensis* (Figure 6A, far right), the predominant sodiated pseudomolecular ion at *m*/*z* 778 is similarly consistent with a structure having (4*E*,8*E*)-*N*-2′-hydroxyalkanoyl-9-methyl-4,8-sphingadienine as the ceramide moiety. In a $^{+}$ESI-MS/CID-MS experiment with selection of the pseudomolecular ion in Q1 (not shown), abundant Ω and T fragments at *m*/*z* 496 and 348, respectively, confirmed that the fatty acyl group is 2-OH-octadec*an*oate (h18:0), and (d19:2) 9-methylsphinga-4,8-dienine again is the long-chain base. $^{+}$ESI-MS/CID-MS fragment data and interpretations are summarized for the GalCer fraction from *A. fumigatus* and for the GlcCer fraction from the yeast form of *P. brasiliensis* in Table 4 and Scheme 2.

The GlcCer fractions from *A. fumigatus* and from the mycelium form of *P. brasiliensis* showed similar pseudomolecular ion profiles (Figure 6A, middle left and right, respectively), each having *m*/*z* 776 and 778 in similar abundance, consistent with mixtures containing both ceramide types (h18:1 and h18:0). Considering that the M+2 ^{13}C isotope satellite peak from *m*/*z* 776 contributes a small increment to the abundance of *m*/*z* 778, it appears from these spectra that the unsaturated fatty acid form is present in a slight excess in each fraction. However, precise quantitation from these spectra is not practical without knowing whether the ionization efficiencies of the two species are comparable under the conditions of analysis. This would require calibration with mixtures of known composition. $^{+}$ESI-MS/CID-MS experiments with selection of either *m*/*z* 776 or 778 (not shown) confirmed that the difference between the two species is in the fatty acid, since the same abundant Ω fragment at *m*/*z* 496 is produced in each case, while the T fragments differed by 2 u, depending on the *m*/*z* of the precursor.

Fatty Acid Analysis. The fatty acid composition of each cerebroside fraction was analyzed by GC-EI/MS of TMS-FAMES after acid-catalyzed methanolysis and trimethylsilylation. Authentic 2-hydroxyoctadecanoic acid methyl ester was used as a standard with respect to retention time and mass spectrum. Incomplete separation of methyl-2-hydroxyoctadecanoate and -enoate derivatives in the system used, along with a lack of a standard for the latter with which to calculate a relative response factor, again made quantitation somewhat problematic. Nevertheless, based on peak retention times and identification of components based on EI-MS

[3] Previously, Gu et al. (*71*) reported a $^{+}$ESI-MS/CID-MS experiment on (*E*)-Δ^3-unsaturated GlcCer from *A. fumigatus*; their spectrum, in which the ion selected in Q1 was apparently $[MH - H_2O]^+$ (*m*/*z* 736), differed fundamentally from that shown in Figure 6A, particularly with respect to the ions characteristic for sphingosine and fatty acyl chain length (no ions analogous to those at *m*/*z* 346 and 496 were apparent).

Table 4: $^{+}$ESI-MS and $^{+}$ESI-MS/CID-MS Data ($+Na^+$) for GalCer of *A. fumigatus* and GlcCer of Yeast Form *P. brasiliensis*, with Proposed Interpretations of Fragments (All Values Nominal, Monoisotopic *m*/*z*)[a]

interpretation (all $+Na^+$)	*A.f.* GalCer	*P.b.*Yeast GlcCer
M	776	778
$M-H_2O$	758	760
Y_0	614	616
Z_0	596	598
Z_0'	578	580
I	524	524
I′	506	506
Ω (≡M−acyl)	**496**	**496**
Ω′ (≡M−acyl−H_2O)	478	478
?	468	468
Z_0/H	416	418
T [S] (≡Z_0/G)	**346**	**348**
O′ [W′]	316	316
O″ [W″]	298	298
E	244	244
C_1	203	203
β_1	185	185
?	157	157
$^{0,2}A_1-CH_2O$	113	113

[a] Fragment nomenclature is after Costello et al. (*65*−*67*) as modified and expanded by Ann and Adams (*46*, *68*); for additional designations, see text and Scheme 2. Square bracketed designations refer to Costello designations where modified. Key abundant ions giving the mass of sphingosine alkyl and fatty acyl moieties are emphasized by boldface.

Scheme 2: Fragmentation Nomenclature Used for Cationized Cerebrosides in Low-Energy $^{+}$ESI-MS/CID-MS[a]

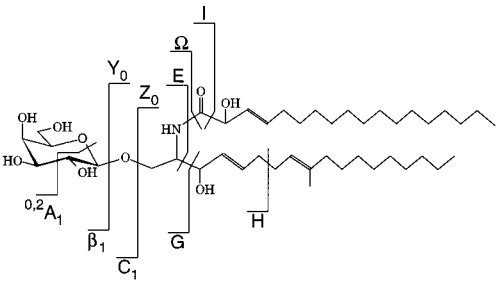

[a] After Costello et al. (*65*−*67*) and Ann and Adams (*46*, *68*). $\beta_1 \equiv B_1$; Ω ≡ is a proposed designation for M−acyl, which is analogous to the ion previously designated as W (*67*) or O (*68*), except that the Hex moiety is retained.

(difference of 2 u in *m*/*z* for $[M^{\bullet}-15]^+$ and $[M^{\bullet}-59]^+$ between the two fatty acid derivatives), it was verified that these cerebroside fractions contained 2-hydroxyoctadec*en*oate and 2-hydroxyoctadec*an*oate in amounts ranging from almost none of the former, in the case of some GlcCer fractions from yeast forms of *P. brasiliensis*, to almost none of the latter, in the case of GalCer fractions from *A. fumigatus* strain 9197. All fractions contained small amounts of nonhydroxylated fatty acids.

DISCUSSION

The results reported here establish a number of significant points concerning the cerebroside composition of *P. brasiliensis*. Like the majority of fungi examined so far, *P. brasiliensis* appears to synthesize only glucocerebrosides, making use of the characteristic (4*E*,8*E*)-9-methyl-4,8-sphingadienine base and, almost exclusively, 18-carbon 2-hydroxy fatty acids for assembly of the ceramide part. Interestingly, a number of marine organisms also synthesize glycosphingolipids utilizing the same or a closely analogous sphingosine moiety, usually in combination with 2-hydroxy fatty acids. Identifications of this sphingosine structure as a novel component of cerebrosides from a fungus, *Fusicoccum amygdali* Delacroix (*47*),[4] and from a sea anemone, *Metridium senile* (*48*), were reported in the same year. Some marine sponge and sea star species add a characteristic (*E*)-Δ^{10}-unsaturation to this basic sphingosine skeleton (*49*−*53*).

The (*E*)-Δ^3-unsaturation of the 2-hydroxy fatty acid, on the other hand, appears so far to be a modification exclusive to fungal cerebrosides. It was detected for the first time in a cerebroside from *A. oryzae* (*28*), and later from *F. amygdali* Del. (*47*). A number of fungi utilize both saturated and (*E*)-Δ^3-unsaturated 2-hydroxy fatty acids, either variable or relatively homogeneous with respect to chain length, in cerebroside synthesis. However, this report is the first instance of a clear difference in the amount of (*E*)-Δ^3-unsaturation correlated with the growth phase of a dimorphic fungus. Matsubara et al. (*24*) characterized glucocerebrosides from both yeast and mycelial forms of the mycopathogen *C. albicans*, but reported no difference in ceramide composition between the two. Whether the difference noted in *P. brasiliensis* is a more general phenomenon characteristic of taxonomically related, thermally dimorphic mycopathogens remains to be tested. The possible function of such a chemical dimorphism is unclear, but one possibility is that *P. brasiliensis* requires a higher percentage of (*E*)-Δ^3-unsaturation in its cerebroside fraction to maintain proper membrane characteristics for the conversion to, and/or maintenance of, the low-temperature mycelial form. However, compared with the effects of midchain unsaturation, a modification often found in mammalian ceramide- and diacylglycerol-based lipids, the effects of (*E*)-Δ^3-unsaturation on membrane properties may be considerably smaller. Midchain fatty acyl unsaturation, usually in the (*Z*) configuration, is known to increase the cross-sectional area of a lipid; the permanent kink formed in the hydrocarbon chain has a powerful disorganizing effect which inhibits packing of the lipid in the gel state (*54*). The result is a destabilization of the gel state and a consequent lowering of the phase transition temperature compared with a fully saturated homolog. In contrast, the effect of (*E*)-Δ^3-unsaturation on the conformation of the ceramide fatty acyl chain may be minimal; from inspection of a crystal structure of cerebroside containing 2-hydroxy fatty acid (*55*), it appears that the (*E*)-Δ^3 double bond could be accommodated without significant repositioning of the acyl chain or consequent changes in packing interactions. However, this does not rule out possible subtle effects occurring in a membrane environment, which could result from restriction of available conformation space or changes in the rate of some conformational transitions.

Another possibility, given the demonstrated activities of fungal cerebrosides in biological assays such as stimulation of fruiting-body formation in *S. commune* (*16*, *17*, *30*), is that the (*E*)-Δ^3 modification of *P. brasiliensis* cerebroside serves a specific messenger function in the yeast to mycelial conversion. The activation (or deactivation) of a desaturase responsible for this modification could thus be one step in a signaling cascade controlling the transition from yeast to mycelium (or the reverse) which is initiated by a change in temperature. Alternatively, control of the (*E*)-Δ^3 desaturase activity might take place at the transcription level. Studies in both mammalian cells and *Saccharomyces cerevisiae* have shown that free ceramides, as well as further products of sphingolipid turnover, such as sphingosines and their derivatives, may serve as potent modulators of cellular function and behavior (*14*, *56*−*58*).[5] Consistent with this, Kawai and Ikeda reported (*16*, *17*, *21*) that ceramides generated by removal of the saccharide moiety from fungal cerebrosides maintained their potency in fruiting-body-inducing assays. Thus, in this case, it is possible that the active substance in vivo is the metabolic product of cerebroside with a fungal β-glucoceramidase.

An interesting parallel dimorphism was observed previously (*9*) with respect to the glycan moieties of GIPCs expressed by *P. brasiliensis*. Quantitative analysis of the two major GIPCs found in both forms, Pb-**1** (band 1) and Pb-**2** (band 2), showed that while the mycelium form expressed Pb-**1** in slight excess (58% in two different strains, B339 and Pb18), the yeast form expressed Pb-**1** in much higher proportion (91% and 94% in strains B339 and Pb18, respectively). Overall, the mycelium forms appeared to contain more total GIPC by weight than the yeast forms ($>2\times$ for strain Pb18). Subsequently, the structures of Pb-**1** and Pb-**2** were fully characterized as Man*p*α1→3[Gal*f*β1→6]-Man*p*α1→2Ins1-P-1Cer and Man*p*α1→3Man*p*α1→2Ins1-P-1Cer, respectively (*33*). Thus, changes in the equilibrium of synthesis and degradation of polysaccharides and structural proteins of the fungal cell wall, which are proposed to be essential factors for the maintenance of yeast and mycelial morphologies in *P. brasiliensis*, as well as for promoting late stages of morphological transitions (*59*), are accompanied

[4] Although Ballio et al. (*47*) assigned the *Z* configuration to the Δ^4 double bond and left the geometry of the Δ^8 double bond unspecified, Kawai et al. (*21*) have proposed that the configurations are 4*E*,8*E* as found in other fungi.

[5] Interestingly, while a great deal has been learned about the biosynthesis and functional roles of glycosphingolipids through studies with *Saccharomyces cerevisiae* [for a recent review, see Dickson (*14*)], the class of cerebrosides discussed here have never been observed in this yeast, and therefore *Saccharomyces* would appear to be unsuitable as a model for their study [except, possibly, for analyzing element(s) in the biosynthetic pathway which might have been lost or inactivated through evolution].

by changes in cell membrane glycosphingolipid metabolism. The possibility that glycosphingolipids can modulate the activity of membrane-bound enzymes (*60*, *61*) suggests that they could play a significant role in dimorphism through their interaction with one or more key enzymes affecting fungal morphology. This is an especially appealing idea since the major cell wall biosynthetic enzymes, chitin synthase and glucan synthases, are membrane-bound (*62*).

The availability of detailed structures of both GIPCs and cerebrosides from *P. brasiliensis* points in addition to a remarkable dichotomy in the utilization of two distinct types of ceramides in different biosynthetic pathways. Unlike the cerebrosides characterized here, the ceramide components of *P. brasiliensis* GIPCs were previously found to consist almost exclusively of unbranched (t18:0) 4-hydroxysphinganine (phytosphingosine), in combination with saturated 2-hydroxy fatty acids (predominantly h24:0) (*33*). This partitioning of ceramide types into distinct catabolic pathways most likely results either from compartmentalization of their biosynthesis and/or transport, or from selective recognition of ceramide structural elements somewhat remote from the reaction site by both the putative ceramide β-glucosyltransferase and the IPC synthase (*63*). A similar partitioning of ceramides is apparent between the cerebroside and (G)IPC fractions of *C. albicans* (*24*, *64*) and *A. fumigatus* (Toledo, M. S., Levery, S. B., Straus, A. H., and Takahashi, H. K., unpublished observations).

With respect to the amounts of (*E*)-Δ^3 modification observed in gluco- and galactocerebrosides of *A. fumigatus*, although Villas Boas et al. have reported (*22*) on the existence of both GlcCer- and GlcCer/GalCer-producing strains of *A. fumigatus*, the presence of 2-OH-octadec*an*oate (h18:0) in any of these cerebrosides was not previously noted. Since the strains used in the present work (237; ATCC 9197) are different from either of those used in their studies (NCPF strains 2109 and 2140), it is possible that production of cerebrosides containing 2-OH-octadecanoate in *A. fumigatus* is, like the expression of galactocerebrosides, a strain-dependent phenomenon. The differences noted between the two strains used in our studies support this view; since the level of GalCer in strain 237 was found to be considerably lower than in 9197, it follows that the overall level of (*E*)-Δ^3-unsaturation represented by the combined GlcCer/GalCer fractions in strain 237 must also be much lower than in 9197. Further, while the precise mechanism for this partitioning of (*E*)-Δ^3-unsaturated ceramide with respect to hexose structure is unclear, the results from all three strains expressing GalCer (2109, 9197, 237) are consistent with a galactosyltransferase less efficient at utilizing the saturated form of this ceramide as its acceptor substrate while, on the other hand, the glucosyltransferase may use both forms equally well. If this were indeed the case, one would expect reduced levels of available (*E*)-Δ^3-unsaturated substrate to favor synthesis of GlcCer in higher proportions, as found with strain 237. To account for the results with strains such as 2140, which produce only glucocerebroside (*22*), a different mechanism may also be available for switching the galactosyltransferase off altogether. The possible biological significance for producing such differences in *A. fumigatus* cerebroside patterns seems, at present, obscure, but the ability to vary both saccharide and ceramide structural features may be one factor in the ability of this fungus to adapt to a wide range of substrates and growth conditions, as well as a variety of host organisms and tissues.

ACKNOWLEDGMENT

We gratefully acknowledge the technical assistance of Rebecca Lindsey, Ian Taylor, and Ben Favis.

REFERENCES

1. Beninger, P., Dismukes, W. E., Edwards, J. E., Fonzi, W., Galgiani, J. N., Hector, R., Pfaller, M., and Wong, B. (1994) The Second NIAID Workshop in Medical Mycology: Molecular and Immunologic Approaches to the Diagnosis and Treatment of Systemic Mycosis, University of Arizona, Flagstaff, AZ.
2. Dixon, D. M., Cox, R., Cutler, J., and Deepe, G. (1995) The Third NIAID Workshop in Medical Mycology: Immunology in Medical Mycology: Antigenic Peptides, Glycobiology, and Vaccines, Yellowstone Conference Center, Big Sky, MT.
3. Casadevall, A., Dixon, D. M., Kozel, T. R., Murphy, J. W., Sobel, J. D., and Tuttleman, M. (1997) The Fourth NIAID Workshop in Medical Mycology: Host Response to Fungi, University of Nevada, Reno, NV.
4. Straus, A. H., Freymuller, E., Travassos, L. R., and Takahashi, H. K. (1996) *J. Med. Vet. Mycol. 34*, 181−186.
5. Hearn, V. M., and Mackenzie, D. W. (1989) in *Immunology of Fungal Diseases* (Kurstak, E., Marquis, G., Auger, P., de Repentigny, L., and Montplaisir, S., Eds.) pp 87−111, Marcel Dekker, Inc., New York.
6. San-Blas, G., and San-Blas, F. (1989) in *Immunology of Fungal Diseases* (Kurstak, E., Marquis, G., Auger, P., de Repentigny, L., and Montplaisir, S., Eds.) pp 171−192, Marcel Dekker, Inc., New York.
7. Barr, K., and Lester, R. L. (1984) *Biochemistry 23*, 5581−5588.
8. Barr, K., Laine, R. A., and Lester, R. L. (1984) *Biochemistry 23*, 5589−5596.
9. Toledo, M. S., Suzuki, E., Straus, A. H., and Takahashi, H. K. (1995) *J. Med. Vet. Mycol. 33*, 247−251.
10. Levery, S. B., Toledo, M. S., Suzuki, E., Salyan, M. E., Hakomori, S., Straus, A. H., and Takahashi, H. K. (1996) *Biochem. Biophys. Res. Commun. 222*, 639−645.
11. Straus, A. H., Suzuki, E., Toledo, M. S., Takizawa, C. M., and Takahashi, H. K. (1995) *Braz. J. Med. Biol. Res. 28*, 919−923.
12. Kannagi, R., and Hakomori, S. (1986) in *Handbook of Experimental Immunology* (Weir, D. M., Herzenberg, L. A., and Blackwell, C. C., Eds.) pp 117.1−117.20, Blackwell, Oxford.
13. Li, R., Villacreses, N., and Ladisch, S. (1995) *Cancer Res. 55*, 211−214.
14. Dickson, R. C. (1998) *Annu. Rev. Biochem. 67*, 27−48.
15. Daum, G., Lees, N. D., Bard, M., and Dickson, R. (1998) *Yeast 14*, 1471−1510.
16. Kawai, G., and Ikeda, Y. (1985) *J. Lipid Res. 26*, 338−343.
17. Kawai, G., and Ikeda, Y. (1983) *Biochim. Biophys. Acta 754*, 243−248.
18. Fogedal, M., Mickos, H., and Norberg, T. (1986) *Glycoconj. J. 3*, 233−237.
19. Kawai, G. (1989) *Biochim. Biophys. Acta 1001*, 185−190.
20. Sawabe, A., Morita, M., Okamoto, T., and Ouchi, S. (1994) *Biol. Mass Spectrom. 23*, 660−664.
21. Kawai, G., Ikeda, Y., and Tubaki, K. (1985) *Agric. Biol. Chem. 49*, 2137−2146.
22. Villas Boas, M. H., Egge, H., Pohlentz, G., Hartmann, R., and Bergter, E. B. (1994) *Chem. Phys. Lipids 70*, 11−19.
23. Sitrin, R. D., Chan, G., Dingerdissen, J., DeBrosse, C., Mehta, R., Roberts, G., Rottschaefer, S., Staiger, D., Valenta, J., Snader, K. M., Stedman, R. J., and Hoover, J. R. E. (1988) *J. Antibiot. (Tokyo) 41*, 469−480.
24. Matsubara, T., Hayashi, A., Banno, Y., Morita, T., and Nozawa, Y. (1987) *Chem. Phys. Lipids 43*, 1−12.

25. Duarte, R. S., Polycarpo, C. R., Wait, R., Hartmann, R., and Bergter, E. B. (1998) *Biochim. Biophys. Acta 1390*, 186−196.
26. Mizushina, Y., Hanashima, L., Yamaguchi, T., Takemura, M., Sugawara, F., Saneyoshi, M., Matsukage, A., Yoshida, S., and Sakaguchi, K. (1998) *Biochem. Biophys. Res. Commun. 249*, 17−22.
27. da Silva Bahia, M. C., Vieira, R. P., Mulloy, B., Hartmann, R., and Bergter, E. B. (1997) *Mycopathologia 137*, 17−25.
28. Fujino, Y., and Ohnishi, M. (1976) *Biochim. Biophys. Acta 486*, 161−171.
29. Wagner, H., and Fiegert, E. (1969) *Z. Naturforsch. B 24*, 359.
30. Kawai, G., and Ikeda, Y. (1982) *Biochim. Biophys. Acta 719*, 612−618.
31. Braunschweiler, L., and Ernst, R. R. (1983) *J. Magn. Reson. 53*, 521−528.
32. Cardoso, D. B. S., Angluster, J., Travassos, L. R., and Alviano, C. S. (1987) *FEMS Microbiol. Lett. 43*, 279−282.
33. Levery, S. B., Toledo, M. S., Straus, A. H., and Takahashi, H. K. (1998) *Biochemistry 37*, 8764−8775.
34. Straus, A. H., Levery, S. B., Jasiulionis, M. G., Salyan, M. E., Steele, S. J., Travassos, L. R., Hakomori, S., and Takahashi, H. K. (1993) *J. Biol. Chem. 268*, 13723−13730.
35. Suzuki, E., Toledo, M. S., Takahashi, H. K., and Straus, A. H. (1997) *Glycobiology 7*, 463−468.
36. Sweeley, C. C. (1969) *Methods Enzymol. 14*, 254−267.
37. Dabrowski, J., Hanfland, P., and Egge, H. (1980) *Biochemistry 19*, 5652−5658.
38. Yamada, A., Dabrowski, J., Hanfland, P., and Egge, H. (1980) *Biochim. Biophys. Acta 618*, 473−479.
39. Dabrowski, J., Egge, H., and Hanfland, P. (1980) *Chem. Phys. Lipids 26*, 187−196.
40. Bax, A., and Davis, D. G. (1985) *J. Magn. Reson. 65*, 355−360.
41. Davis, A. L., Keeler, J., Laue, E. D., and Moskau, D. (1992) *J. Magn. Reson. 98*, 207−216.
42. Bodenhausen, G., and Ruben, D. J. (1980) *Chem. Phys. Lett. 69*, 185−189.
43. Bax, A., and Summers, M. F. (1986) *J. Am. Chem. Soc. 108*, 2093−2094.
44. Bax, A., and Marion, D. (1988) *J. Magn. Reson. 78*, 186−191.
45. Saito, T., and Hakomori, S. (1971) *J. Lipid Res. 12*, 257−259.
46. Ann, Q., and Adams, J. (1993) *Anal. Chem. 65*, 7−13.
47. Ballio, A., Casinovi, C. G., Framondino, M., Marino, G., Nota, G., and Santurbano, B. (1979) *Biochim. Biophys. Acta 573*, 51−60.
48. Karlsson, K.-A., Leffler, H., and Samuelsson, B. E. (1979) *Biochim. Biophys. Acta 574*, 79−93.
49. Jin, W., Rinehart, K. L., and Jares-Erijman, E. A. (1994) *J. Org. Chem. 59*, 144−147.
50. Costantino, V., Fattorusso, E., and Mangoni, A. (1995) *Liebigs Ann. 1995*, 1471−1475.
51. Costantino, V., Fattorusso, E., and Mangoni, A. (1995) *Liebigs Ann. 1995*, 2133−2136.
52. Irie, A., Kubo, H., and Hoshi, M. (1990) *J. Biochem. (Tokyo) 107*, 578−586.
53. Natori, T., Morita, M., Akimoto, K., and Koezuka, Y. (1994) *Tetrahedron 50*, 2771−2784.
54. Yeagle, P. (1987) *The Membranes of Cells*, Academic Press, Inc., London.
55. Pascher, I., and Sundell, S. (1977) *Chem. Phys. Lipids 20*, 175−191.
56. Merrill, A. H., Hannun, Y., and Bell, R. M. (1993) *Adv. Lipid Res. 25*, 1−24.
57. Hannun, Y., Obeid, L. M., and Wolff, R. M. (1993) *Adv. Lipid Res. 25*, 43−64.
58. Mathias, S., and Kolesnick, R. (1998) *Adv. Lipid Res. 25*, 65−90.
59. San-Blas, F., and San-Blas, G. (1985) in *Fungal Dimorphism* (Szaniszlo, P. J., and Harris, J. L., Eds.) pp 93−120, Plenum Press, New York and London.
60. Patton, J. L., and Lester, R. L. (1992) *Arch. Biochem. Biophys. 292*, 70−76.
61. Lester, R. L., and Dickson, R. C. (1993) *Adv. Lipid Res. 26*, 253−274.
62. Cabib, E., Bowers, B., Sburlati, A., and Silverman, S. J. (1998) *Microbiol. Sci. 5*, 370−375.
63. Nagiec, M. M., Nagiec, E. E., Baltisberger, J. A., Wells, G. B., Lester, R. L., and Dickson, R. C. (1997) *J. Biol. Chem. 272*, 9809−9817.
64. Steiner, S., Smith, S. W., Waechter, C. J., and Lester, R. L. (1969) *Proc. Natl. Acad. Sci. U.S.A. 64*, 1042−1048.
65. Domon, B., Vath, J. E., and Costello, C. E. (1990) *Anal. Biochem. 184*, 151−164.
66. Costello, C. E., and Vath, J. E. (1990) *Methods Enzymol. 193*, 738−768.
67. Domon, B., and Costello, C. E. (1988) *Biochemistry 27*, 1534−1543.
68. Ann, Q., and Adams, J. (1992) *J. Am. Soc. Mass Spectrom. 3*, 260−263.
69. Koerner, T. A. W., Prestegard, J. H., Demou, P. C., and Yu, R. K. (1983) *Biochemistry 22*, 2676−2687.
70. Koerner, T. A. W., Prestegard, J. H., Demou, P. C., and Yu, R. K. (1983) *Biochemistry 22*, 2687−2690.
71. Gu, M., Kerwin, J. L., Watts, J. D., and Aebersold, R. (1997) *Anal. Biochem. 244*, 347−356.

BI982898Z